Dyes and Pigments 88 (2011) 57–64

Contents lists available at ScienceDirect

Dyes and Pigments

journal homepage: www.elsevier.com/locate/dyepig

Novel D–π_3–$(A)_{1-3}$ multibranched chromophores as an efficient two-photon-induced polymerization initiator

Xiaomei Wang [a,*], Feng Jin [c], Weizhou Zhang [a], Xutang Tao [b], Xuan-Ming Duan [c,*], Minhua Jiang [b]

[a] Institute of Chemistry and Bioengineering, Suzhou University of Science and Technology, Suzhou 215009, China
[b] State Key Laboratory of Crystal Materials, Shandong University, Jinan 250100, China
[c] Laboratory of Organic NanoPhotonics and Key Laboratory of Photochemical Conversion and Functional Materials, Technical Institute of Physics and Chemistry, Chinese Academy of Sciences, Beijing 100190, China

ARTICLE INFO

Article history:
Received 14 February 2009
Received in revised form
28 April 2010
Accepted 5 May 2010
Available online 20 May 2010

Keywords:
Two-photon absorption
Dipolar moment change ($\Delta\mu_{ge}$)
Two-photon-induced polymerization
D–π_3–$(A)_{1-3}$ initiator
Fluorescence quenching
Intermolecular charge-transfer

ABSTRACT

The ability of novel branched chromophores that contained a triphenylamine group as donor, naphthalene as π-bridge and pyridyl as acceptor group, to act as two-photon absorption and two-photon induced polymerization initiators were investigated. Linear and nonlinear optical spectra revealed that chromophores with large dipolar moment change gave strong intramolecular charge-transfer characteristics that exhibited enhanced two-photon absorption cross-section. A variety of micro-objects were fabricated, using an acrylate matrix, that contained the novel chromophores as two-photon induced polymerization initiator. Molecular energy levels, electrochemistry and linear absorption spectra, as well as one-photon fluorescence quenching measurements supported the hypothesis that two-photon induced polymerization proceeds via intermolecular charge-transfer from initiator to monomer and, that the chromophore firstly generates the exciton via two-photon absorption and then transfers charge to the acrylate monomer which then polymerises.

1. Introduction

Two-photon-induced polymerization (TPP) is an attractive technology for 3D-nanostructures and 3D-lithography for photonic crystals, optical data storage, micro-electromechanical systems (MEMS), optical integrated circuits and self-writing waveguides [1–8]. These technologies take advantage of the fact that two-photon absorption (TPA) probability depends quadratically on excitation intensity, resulting in high resolution and deep penetration [9]. Thus, whilst effective TPP initiators of large TPA cross-section have been the subject of much research [1,10–15] over the past decade or so. Improvement in initiation efficiency is required, as well as a deeper understanding of the dependence of this efficiency on molecular parameters. At present, many papers concern both the synthesis and TPP applications of initiators of D-π-D, A-π-A, D–π–A–π–D and A–π–D–π–A architecture [1,10–19]. However, to our knowledge, few reports have systematically studied TPP initiators with D–π_3–$(A)_n$ structure. An increase in dimensionality of donor-π-acceptor molecules appears as a reasonable approach to generate improved TPA cross section in comparison with their linear counterparts [20], this being one way of enhancing the TPP efficiency of initiators. In contrast, chromophores with branched architecture and more acceptor groups usually possess low fluorescence yield, which might contribute to high triplet quantum yield and result in high initiator sensitivity [21–24]. Based on these considerations, novel, D–π_3–$(A)_{1-3}$ chromophores, where "D," "π" and "A" are a triphenylamine group, naphthalene group and pyridyl, respectively were synthesized namely PN-**1**, PN-**2** and PN-**3** (Fig. 1), the three compounds varting in the number of constituent pyridyl units.

2. Experimental

2.1. Measurements

Electron impact (Mode laser) mass spectra and EI mass spectra were obtained on a 4700 Proteome Analyzer (MALDI-TOF-TOF) produced by ABI Company and on an HP 5989 mass spectra instrument, respectively. Hydrogen and carbon nuclear magnetic resonance spectra were determined on a GCT-TOF NMR spectrometer. Element analyses were performed on Perkin 2400(II) autoanalyzer.

Linear absorption measurements of dilute solution were measured with Hitachi U-3500 recording spectro-photometer from quartz curettes of 1 cm path. Steady-state fluorescence and the

* Corresponding authors. Tel.: +86 512 62092786; fax: +86 512 67246786
E-mail addresses: wangxiaomei@mail.usts.edu.cn (X. Wang), xmduan@mail.ipc.ac.cn (X.-M. Duan).

0143-7208/$ – see front matter © 2010 Elsevier Ltd. All rights reserved.
doi:10.1016/j.dyepig.2010.05.001

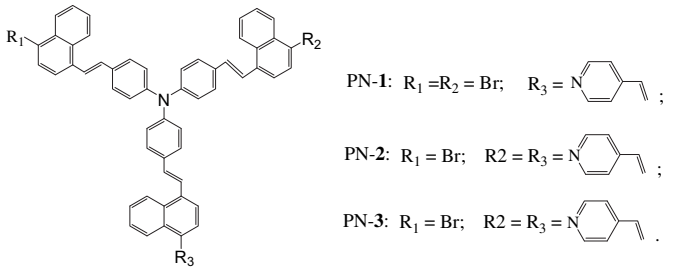

Fig. 1. Molecule structures of new D–π_3–$(A)_{1-3}$chromophores: PN-**1**, PN-**2** and PN-**3**.

time-resolved decay curves were measured on an Edinburgh FLS 920 fluorophotometer equipped with the Xe lamp and a time-correlated single-photon counting (TCSPC) card. Lifetime values were measured by reconvolution fit analysis of the decay profiles with the aid of nF900 software, and the fitting results were judged by the reduced χ^2 value. For one-photon absorption and fluorescence measurements, the concentration of sample in THF solution was 1×10^{-5} mol dm^{-3} and the one-photon fluorescence (OPF) quantum yield (Φ) was measured using fluorescein (in 0.1 mol dm^{-3} aqueous NaOH) as a standard.

Two-photon absorption (TPA) cross-section (δ_{TPA}) of chromophore solution (in THF) was determined by two-photon fluorescence (TPF) method. The light source is a Tsunami mode-locked Ti:sapphire system (700–880 nm, 80 MHz, <130 fs). TPF spectra were recorded by a fiber spectra meter (Ocean Optics USB2000 CCD). The TPA cross-section was determined based on Eq. (1) [25],

$$\delta_s = \delta_{ref}\frac{\phi_{ref}}{\phi_s}\frac{F_s}{F_{ref}}\frac{n_{ref}}{n_s}\frac{c_{ref}}{c_s} \quad (1)$$

where the subscripts of "ref" and "s" stand for reference and sample, respectively. The terms *n* and *c* are the refractive index and the concentration of the solution. The symbols Φ and *F* represent the OPF quantum yield and TPF integral, respectively. For eliminating the disturbance from other photophysical or photochemical processes, the intensity of input pulses was confined within 0.5–2 GW/cm^2 in our experiment. The experimental uncertainty amounts to 10%. Noted that our two-photon fluorescence signal is picked up by an external optical fiber, different from the setup reported previously [22]. Thus, the measured two-photon spectra in this paper are only the approximations.

Cyclic voltammogram of chromophores in deoxygenated dichloromethane was obtained in a three-electrode cell with a platinum counter electrode, a glass carbon working electrode and an Ag/AgCl (0.1 M) reference. The HOMO (highest occupied molecular orbital) energy level relative to vacuum level was calculated using the oxidation potential (after being converted to the potential relative to the standard hydrogen electrode potential, NHE). The band gap (ΔE) was obtained from linear absorption spectra (absorption edge) of chromophores, while the LUMO (lowest unoccupied molecular orbital) energy level was calculated from the ΔE value and the HOMO [26].

2.2. Two-photon initiated photopolymerization

Photocurable acrylate monomer was prepared by mixing methyl acrylate (monomer) and dipentaerythritol hexaacrylate (cross-linker) in almost equal quantity (48/52, W/W). Then, 0.2 wt% of D–π_3–$(A)_n$–chromophore was added as a photoinitiator and a little chloroform was used in order to control the viscosity and increase the compatibility. A laser beam from a mode-locked Ti: sapphire laser system (Tsunami, Spectra-Physics) with the wavelength of 800 nm, a pulse width duration of 80 fs and a repetition rate of 80 MHz was used for all TPP experiments here. The beam was tightly focused into a photoresist on a glass cover slip with an oil-immersion objective lens (100×, numerical aperture = 1.4, Olympus). The acrylate resin was scanned by the focused beam in the *x*–*y* plane by a two-galvanomirror set (HurrySCAN 14, SCANLAB), and along the *z*-axis by a piezostage (P-622.ZCL, PI), both controlled by a computer. After laser fabrication, the unpolymerized monomer was washed out using ethanol. The obtained microstructures were characterized with scanning electron microscopy (SEM; Hitachi S-4300FEGd).

2.3. Synthesis

2.3.1. Tris(4-(2-(4-Bromonaphthalen-1-yl)vinyl)phenyl) amine (TBPA)

Tris-(4-formyl-phenyl) amine [27,28] (1.0 g, 3.04 mmol), ((4-bromonaphthalen-1-yl) methyl) triphenylphosphonium (5.12 g, 9.12 mmol) and NaH (0.36 g, 15.0 mmol) in the presence of 1,4-dioxane and triethylamine (80: 80 V/V) were refluxed for 6 h. After cooling to room temperature, the precipitate was filtered and the filtrate concentrated. The residue was purified using a silica gel column (petroleum/ethyl acetate = 3/1) and obtained 1.15 g of TBPA, yield 46%. MS (MALDI) M^+ = 935.0. Element analysis (%): Cald. 69.10; H, 3.87; N, 1.49. Found. 68.73; H, 3.26; N. 1.98. ^{1}H NMR (400 MHz, $CDCl_3$, TMS): δ, ppm 6.47 (d, 6H, benze-H), 7.20 (d, 6H, benze-H), 6.98 (d, 6H, CH=CH), 7.38–7.70 (m, 18H).

2.3.2. 4-((E)-2-(4-Bromonaphthalen-1-yl)vinyl)-N-(4-((E)-2-(4- bromonaphthalen-1-yl)vinyl)phenyl)-N-(4-((E)-2-(4-((E)-2-(pyridin-4-yl)vinyl)naphthalen-1-yl) vinyl)phenyl)benzenamine (PN-**1**)

Under a nitrogen atmosphere, a stirred mixture of 1.0 g (1.07 mmol) of TBPA, 0.5 g (1.64 mmol) of *tri*-o-tolylphosphine, 0.12 mL (1.07 mmol) of vinylpyridine, 0.0048 g of palladium(II) acetate (0.2 mmol) and 10 mL of triethylamine was refluxed for 24 h. The solvent was removed under reduced pressure and the orange residue dissolved in dichloromethane, washed three times with distilled water, and dried with anhydrous magnesium sulfate, before being filtered and concentrated. The resulting solution was purified over silica gel with ethyl acetate–petroleum ether (5:1) as eluent to obtain 0.125 g of PN-**1** with orange color. M. p. 88–89 °C. MS (MALDI) = 962.8 (M^+). Element analysis (%): Cald. C, 76.10; H, 4.40; N, 2.91. Found. C, 76.42; H, 4.21; N, 3.22. IR (KBr): ν, cm^{-1} 1594.28 (m, benzene), 1507.39 (m, benzene), 957.41 (w, trans-CH=CH), 828.06 (w, *p*-substituted), 758.10 (w, *p*-substituted). ^{1}H NMR (400 MHz, $CDCl_3$, TMS): δ 7.10–7.17 (m, 6H, benze-H), 7.20, 7.22 (d, 6H, J = 8.0, benze-H), 7.50, 7.52 (d, 7H, =CH–), 7.54–7.63 (m, 6H, benze-H), 7.74–7.87 (m, 5H, benze-H), 8.12, 8.16 (d, 1H, =CH–), 8.23–8.31 (m, 6H, benze-H), 8.63, 8.64 (d, 4H, J = 4.0, pyridine-H, benze-H). ^{13}C NMR (100 MHz, $CDCl_3$, TMS): δ 120.93, 123.24, 123.72, 124.03, 124.18, 124.24, 124.34, 126.72, 126.72, 127.17, 127.74, 128.53, 129.82, 131.51, 131.70, 131.99, 144.90, 147.01, 150.22.

2.3.3. N-(4-((E)-2-(4-Bromonaphthalen-1-yl)vinyl)phenyl)-4-((E)-2-(4-((E)-2-(pyridin-4-yl) vinyl)naphthalen-1-yl)vinyl)-N-(4-((E)-2-(4-((E)-2-(pyridin-4-yl)vinyl)naphthalen-1-yl)vinyl)phenyl) benzenamine (PN-**2**)

Under a nitrogen atmosphere, 1.0 g (1.07 mmol) of TBPA, 1.0 g (3.2 mmol) of *tri*-o-tolylphosphine, 0.25 mL (2.25 mmol) of vinylpyridine, 0.0096 g of palladium(II) acetate (0.4 mmol) and 20 mL of triethylamine was refluxed using the procedure outlined for the preparation of PN-**1**. The red colored, two-branched PN-**2** was obtained (yield. 46%). M.p. 115 °C. MS (MALDI) = 907.5 (M^+–Br, 100%). Element analysis (%): Cald. C, 82.75; H, 4.90; N, 4.26. Found.

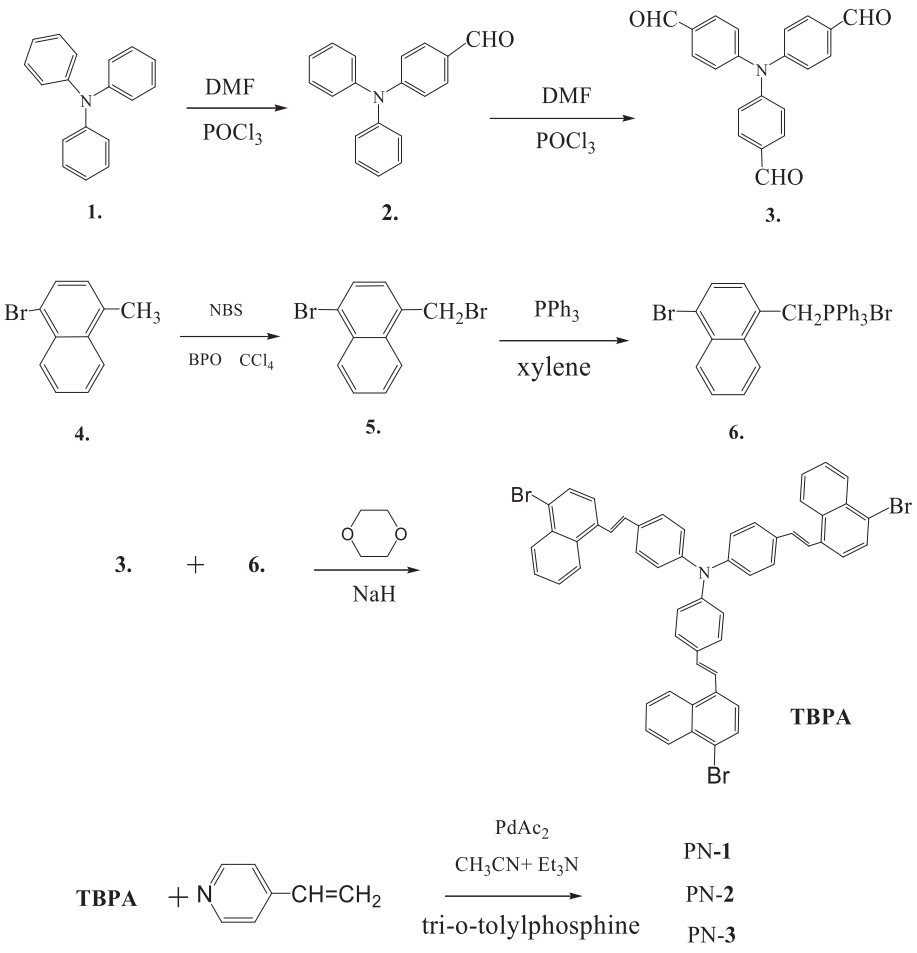

Scheme 1. The synthetic routes of multibranched chromophores PN-**1**, PN-**2** and PN-**3**.

C, 82.36, H, 4.28; N, 4.58. IR (KBr): ν, cm^{-1} 1594.13 (m, benzene), 1504.81 (m, benzene), 959.99 (m, trans-CH=CH), 825.89 (m, *p*-substituted), 760.12 (m, *p*-substituted). ^1H NMR (400 MHz, $CDCl_3$, TMS): δ, ppm 7.11–7.19 (m, 6H, benze-H), 7.22, 7.24 (d, 6H, J = 8.0, benze-H), 7.49,7.50 (d, 8H, =CH–), 7.55–7.64 (m, 10H, benze-H), 7.73–7.89 (m, 6H, benze-H), 8.13, 8.17 (d, 2H, =CH–), 8.25–8.33 (m, 6H, benze-H), 8.64, 8.66 (d, 4H, J = 8.0, pyridine-H). ^{13}C NMR (100 MHz, $CDCl_3$, TMS): δ 121.01, 123.24, 123.80, 124.03, 124.18, 124.29, 124.42, 126.20, 126.42, 126.80, 127.25, 127.82, 128.73, 129.89, 130.30, 131.57, 144.90, 147.01, 150.26.

2.3.4. *Tris(4-(2-(4-(2-(Pyridin-4-yl)vinyl)naphthalen-1-yl)vinyl) phenyl) amine (PN-**3**)*

Under a nitrogen atmosphere, 1.0 g (1.07 mmol) of TBPA, 1.5 g (5.08 mmol) of *tri*-o-tolylphosphine, 0.37 mL (3.3 mmol) of vinylpyridine, 0.01 g of palladium(II) acetate (0.6 mmol) and 35 mL of

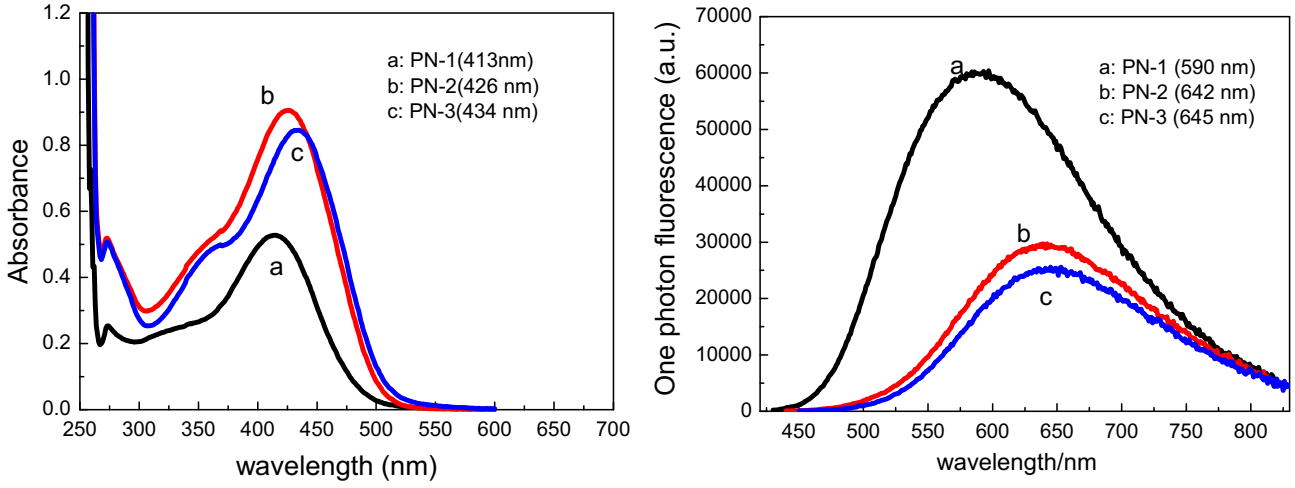

Fig. 2. Linear absorption (left) and fluorescence (right) spectra of D–π_3–$(A)_{1-3}$ chromophores in DMF ($c = 1 \times 10^{-5}$ mol dm^{-3}).

triethylamine was refluxed using the procedure outlined for the preparation of PN-**1**. The red colored three-branched chromophore (PN-**3**) (yield. 40%). M.p. 158 °C. MS (MALDI): M^+ = 1010.4(M^+, 100%), 907.3 (M- vinylpyridine, 20%). Element analysis of (%): Cald. C, 89.08; H, 5.38; N, 5.54. Found. C, 88.58; H, 5.69; N, 5.31. IR (KBr): ν, cm^{-1} 1591.70 (s, benzene), 1504.81 (s, benzene), 957.41 (w, trans-CH=CH), 828.06 (m, *p*-substituted), 763.25 (s, *p*-substituted). ^1H NMR (400 MHz, $CDCl_3$, TMS): δ, ppm 7.10–7.14 (m, 6H, benze-H), 7.22, 7.24 (d, 6H, J = 8.0, benze-H), 7.50,7.51 (d, 9H, =CH–), 7.57–7.63 (m, 12H, benze-H), 7.78–7.88 (m, 6H, benze-H), 8.13, 8.17 (d, 3H, =CH–), 8.24–8.33 (m, 6H, benze-H), 8.63, 8.65 (d, 6H, J = 8.0, pyridine-H). ^{13}C NMR (100 MHz, $CDCl_3$, TMS): δ 121.09, 123.28, 124.06, 124.25, 124.46, 124.55, 126.25, 126.48, 127.87, 128.64, 130.58, 131.57, 132.62, 133.31, 136.27, 145.23, 147.02, 149.98.

3. Results and discussion

3.1. Synthesis

We have successfully synthesized three two-photon absorbing chromophores, denoted as PN-**1**, PN-**2** and PN-**3**, which contain triphenylamine as electron donor, pyridyl ring as electron acceptor, and naphthalene as π-conjugation unit. The synthetic routes of PN-**1**, PN-**2** and PN-**3** are shown in Scheme 1. To achieve synthesis of these chromophores, Vilsmier reaction, Heck-type and Wittig-type condensations have been explored. With *tri*phenylamine (**1**) as the starting material, *4,4′-di*formyl *tri*phenylamine (**2**) and *tris*-(*4*-formylphenyl) amine (**3**) were obtained under the condition of Vilsmier reaction. Then, compound **6** was produced in high yield (80%) by initial bromination and following Wittig reaction, with 1-bromo-4-methylnaphthalene (**4**) as the starting material. Also, by Wittig reaction of **3** with **6**, TBPA was obtained in the bright yellow powders (40%). Finally, the reaction of TBPA and vinylpyridine in the presence of palladium(II) acetate and *tri*-o-tolylphosphine treated in Heck condition produces the object products PN-**1**, PN-**2** and PN-**3**.

3.2. One-photon and two-photon optical properties

Linear absorption spectra of chromophores (see Fig. 2, left), show that the ICT (intramolecular charge-transfer) bands have 13 nm of red-shift from PN-**1** (at 413 nm) to PN-**2** (at 426 nm) and 8 nm of red-shift from PN-**2** to PN-**3** (at 434 nm); meanwhile, the one-photon fluorescence (OPF) spectra, presented in Fig. 2 (right), show the red-shift of 52 nm from PN-**1** (at 590 nm) to PN-**2** (at 642 nm) and of 3 nm from PN-**2** to PN-**3** (at 645 nm). These imply that PN-**2** possesses stronger intramolecuar charge-transfer and delocalized electron-coupling, which have contribution to TPA cross-section [29]. As a result (see Fig. 3a), PN-**2** (162 GM) exhibits rapid enhancement in TPA cross-section, relative to PN-**1** (52 GM) and PN-**3** (165 GM). Moreover, two-photon fluorescence of PN-**2** shows almost as the same as that of PN-**3**, which are the obvious bathochromic shift relative to PN-**1** (see Fig. 3b). We reported that the enhancement in TPA cross-section for triphenylamine-branching chromophore was originated from larger dipole moment change ($\Delta\mu_{ge}$) and strong intramolecular charge-transfer [29]. Thus, the $\Delta\mu_{ge}$ values between the ground- and excited-states for D–π_3–$(A)_n$-chromophores were testified according to Lippert–Mataga relationship (Eq. (2)).

$$\nu_{abs} - \nu_{em} = \frac{\mu_e\left(\Delta\mu_{ge}\right)}{\hbar c\alpha^3}\Delta f + \text{const.} \quad (2)$$

$$\text{with } \Delta f = \frac{\varepsilon - 1}{2\varepsilon + 1} - \frac{n^2 - 1}{2n^2 + 1} \quad (3)$$

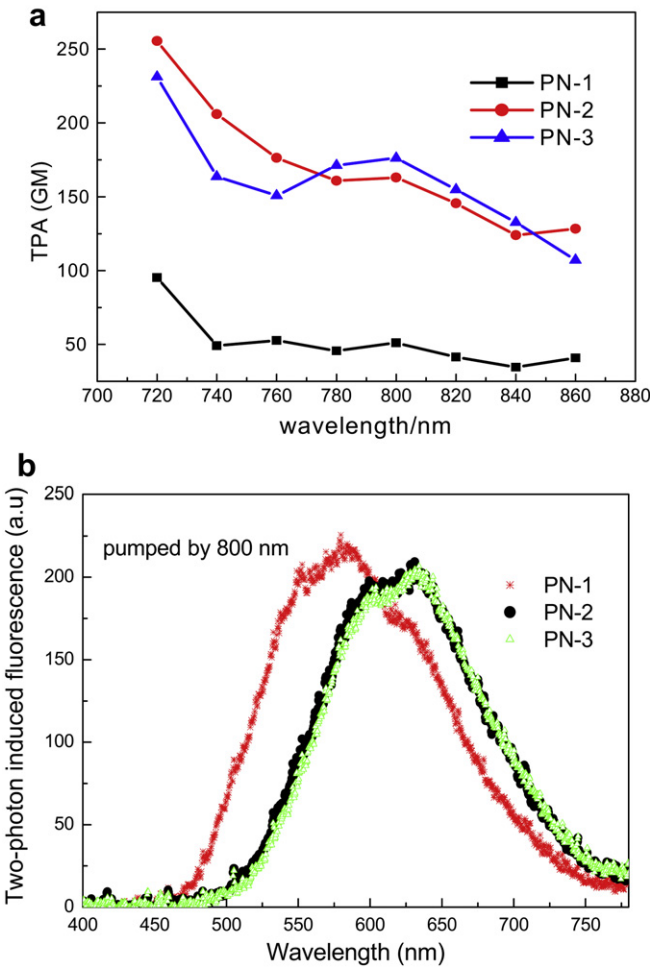

Fig. 3. Two-photon absorption cross-sections (a) and two-photon-induced fluorescence spectra (b) of PN-**1**, PN-**2** and PN-**3** in DMF (1×10^{-4} mol dm^{-3})

In this equation, Stoke's shift ($\nu_{abs} - \nu_{em}$) is related to dipole moment change ($\Delta\mu_{ge}$). The symbols α and c are the molecular size and the light speed, respectively. The symbol $\hbar$ is Plank constant divided by 2π. Orientation polarizability (Δf) of solvent is defined by Eq. (3), wherein ε and n are the dielectric constant and the refractive index of the solvent, respectively. The relationship between Stoke's

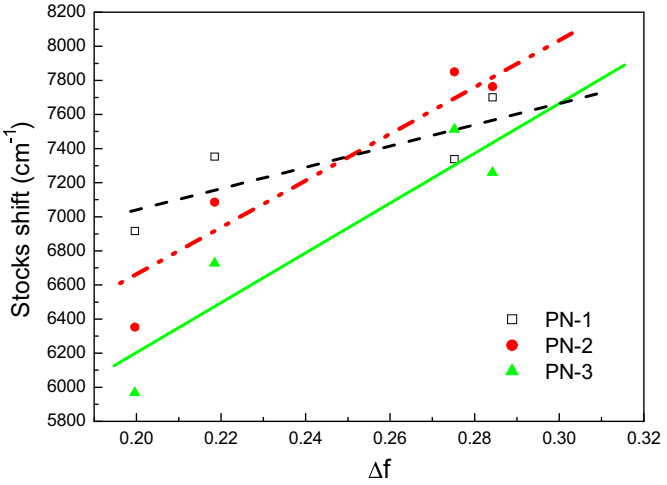

Fig. 4. Relationship between Δf and Stokes shift ($\Delta\nu$) of D–π_3–$(A)_{1-3}$ chromophores.

Table 1
One-photon/two-photon properties, oxidation potential and energy gap of D–π_3–$(A)_{1-3}$ chromophores.

Compd.	λ_{max}^{OPA}(nm)	λ_{max}^{OPF}(nm)	Φ_f	τ_0 (ns)	k_{nf} (10^{-10} s^{-1})	HOMO (eV)	LUMO (eV)	ΔE (eV)	λ_{max}^{TPF}(nm)[a]		δ_{TPA} (GM)[b]
PN-**1**	413	590	0.375	2.42	2.5	−5.61	−3.07	2.54	583	800 (720)	52 (96)
PN-**2**	426	642	0.102	2.42	3.7	−5.59	−3.12	2.47	628	800 (720)	162 (256)
PN-**3**	434	645	0.093	2.43	3.7	−5.59	−3.14	2.45	628	800 (720)	175 (230)

[a] 800 nm laser excitation.
[b] Data in bracket is obtained under the excitation of 720 nm.

shift ($\nu_{abs} - \nu_{em}$) and orientation polarizability (Δf) is presented in Fig. 4, wherein the solid lines represent the fitting results and the slope (k) is in the order of k_3 (PN-**3**) ≈ k_2 (PN-**2**) > k_1 (PN-**1**). Because the size (α) of PN-**1**, PN-**2** and PN-**3** is similar (see Fig. 1), the dipole moment change ($\Delta\mu_{ge}$) should follow the same sequence: $\Delta\mu_{ge}$ (PN-**3**) ≈ $\Delta\mu_{ge}$ (PN-**2**) > $\Delta\mu_{ge}$ (PN-**1**). It was confirmed again that the TPA cross-section is strongly correlative to dipole moment change ($\Delta\mu_{ge}$) and strong intramolecular charge-transfer.

The fluorescence quantum yields (Φ_f), lifetimes (τ) and the nonradiative ($k_{nr} = k_f(1 - \Phi_f)/\Phi_f$) decay rate constants of chromophores are presented in Table 1. As observed, the fluorescence quantum yields reduce from PN-**1** ($\Phi_f = 0.375$) to PN-**2** ($\Phi_f = 0.102$) and to PN-**3** ($\Phi_f = 0.093$). From the point of view of molecular structure, multibranched molecule has more tendency to twisted configuration and might consume more excited energy, which certainly will decrease molecular Φ_f value. Although all chromophores in this study have three branches, the increasing vinylpyridine group, the electron acceptor, on the end of each branch extends molecular chain from PN-**1** to PN-**2,** and to PN-**3** and makes their Φ_f value decrease. On the other hand, calculated nonradiative decay rate constants (k_{nr}) showed the order of PN-**1** (2.5×10^{-10} s^{-1}) < PN-**2** (3.7×10^{-10} s^{-1}) = PN-**3** (3.7×10^{-10} s^{-1}), which might contribute to high triplet quantum yield and usually leads to high initiating sensitivity [23,24].

3.3. Two-photon induced polymerization

As mentioned above, there are two obvious TPA regions beyond 720 nm and 800 nm, and the two-photon-induced polymerization (TPP) experiments were performed with the mode-locked Ti-sapphire femtosecond laser at the wavelength of 800 nm. According to the principle of TPP, the polymerization only occurred near the vicinity of focal point of a beam and the polymerization reaction did not take place in the part out of the laser focus, where the resin could be easily washed out by ethanol. As shown in Fig. 5, the acrylate monomer can be successfully polymerized using our chromophore as initiator, and a variety of micro-objects including micro-ox (15 μm × 10 μm bulk size) and microstereolithography (20 μm × 20 μm bulk size and

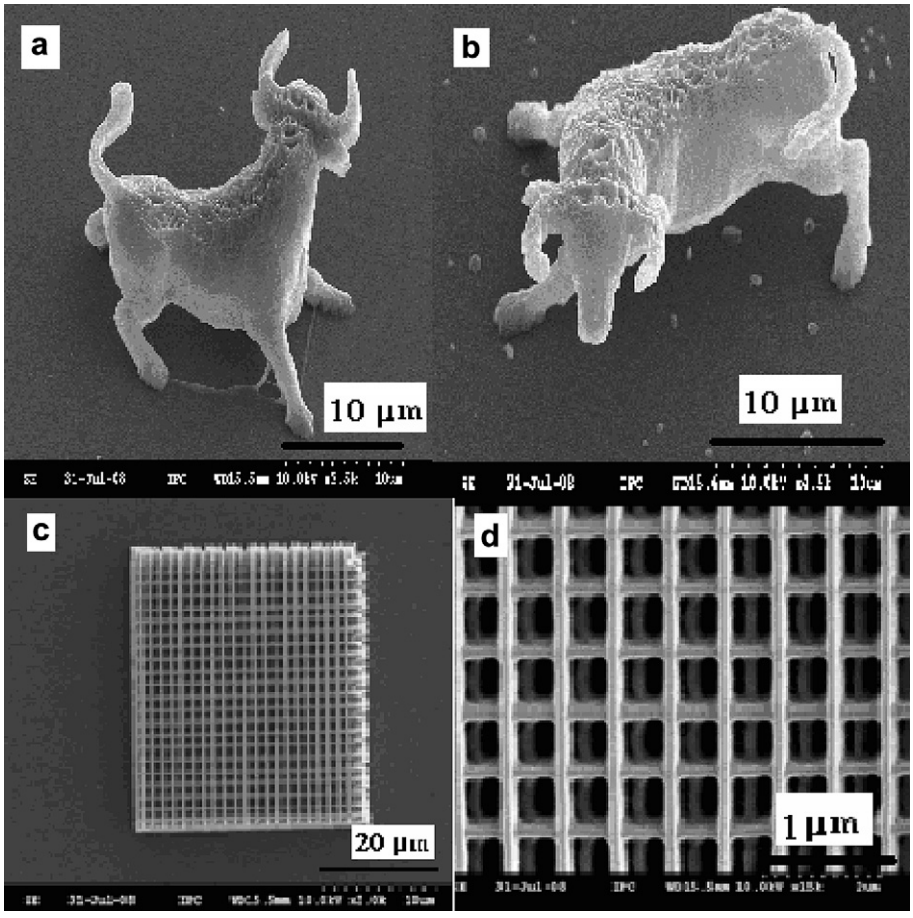

Fig. 5. SEM images of R1 after TPP at the scan speed is 10 μm s^{-1} **a** and **b**: micron ox; **c** and **d**: Logpile structure and the corresponding magnified image, respectively.

Table 2
Components and two-photon-induced polymerization thresholds of resins.

Resin	Initiator	Resin component (wt%)			mol (%)[a]	P_{th}/mW[b]
		MMA	DEP–6A	Initiator		
R1	PN-**1**	48.22	51.58	0.20	0.03	1.4
R2	PN-**2**	48.16	51.64	0.20	0.03	1.3
R3	PN-**3**	48.30	51.50	0.20	0.03	1.3
R4	Benzil	48.35	51.45	0.20	0.17	7.5

[a] Molar ratio of initiator in resin.
[b] Threshold power of initiator in resin. The lowest average laser power, measured before the objective lens, that can guarantee fabricating a solid line with a linear scan speed of 10 μm/s was defined as the threshold of two-photon polymerization (TPP).

1 μm × 1 μm grid size) have been fabricated with spatial resolution of micron and even submicron scale.

In order to investigate the two-photon photosensitivity of chromophores, the threshold power (P_{th}) (defined as the average power before being induced into the objective lens, below which the polymer line cannot be fabricated using a linear scan speed of 10 μm s^{-1}) of polymerization was evaluated by analyzing the polymer lines. The results obtained are presented in Table 2. As can be seen that the P_{th} values of PN-**1**, PN-**2** and PN-**3** are 1.4, 1.3 and 1.3 mW, respectively. Usually, 1–5 wt% of initiator in acrylate monomer have been used for photopolymerization [23]. Here, only 0.2 wt% (0.03 mol%) of chromophores were added in the monomer

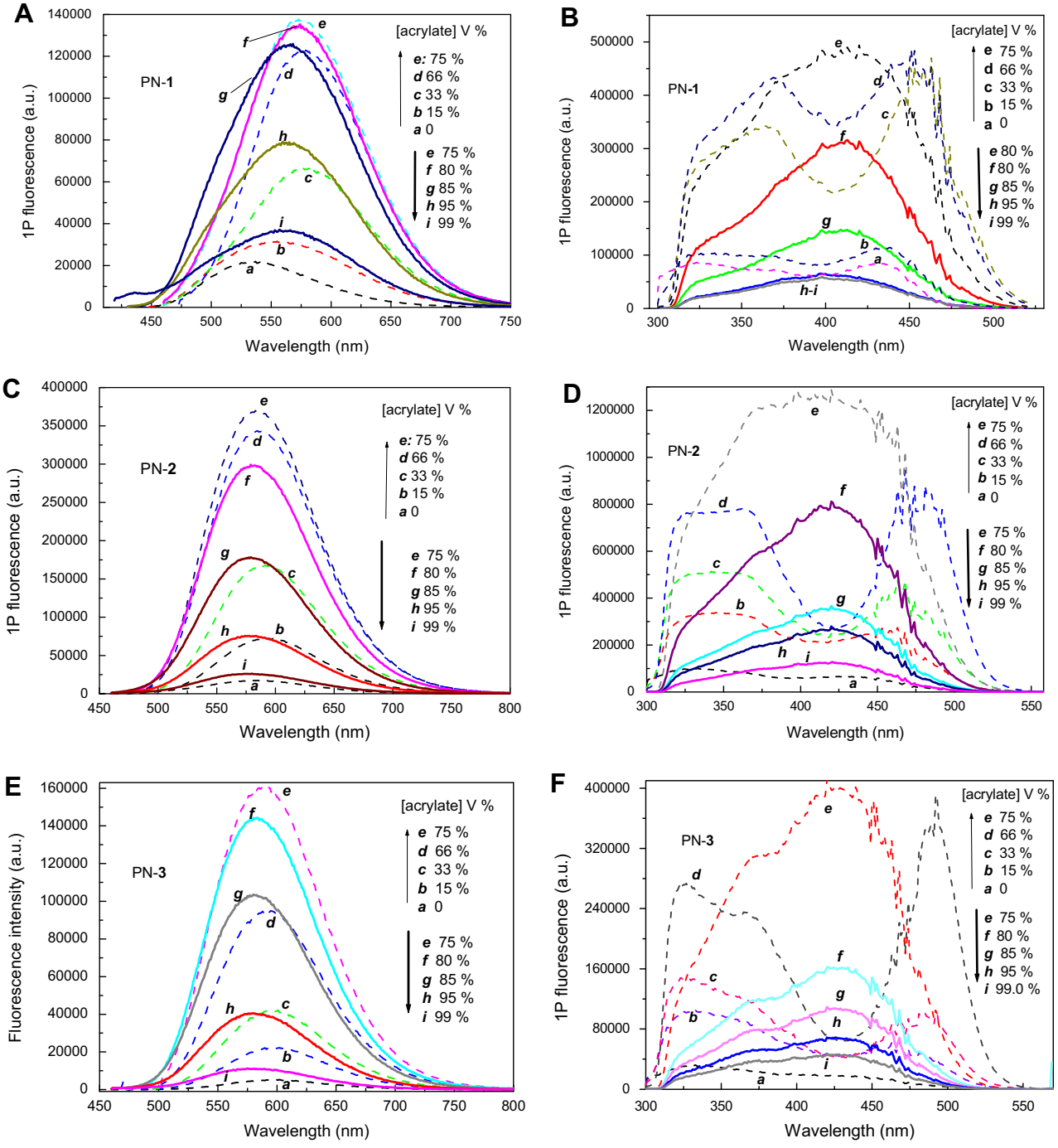

Fig. 6. Fluorescence emission (A, C, E) and fluorescence excitation (B, D, F) spectra of PN-**1**, PN-**2** and PN-**3** in the presence of acrylate monomer with different concentrations [23,24].

(R1–R3) for TPP reaction. Furthermore, in the control experiment, 0.2 wt% (0.17 mol%) of commercial benzil was added in resin (R4) and the threshold power of 7.5 mW was obtained. Evidently, chromophores are efficient TPP photoinitiators in comparison with commercial benzil.

It was reported that the two-photon induced polymerization of acrylate monomer proceeds to a radical mechanism via either energy-transfer or electron-transfer between initiator and monomer [10]. Fluorescence emission and excitation spectra of PN-**1**, PN-**2** and PN-**3** with and without acrylate monomer are presented in Fig. 6(A–F), wherein the changes of intensity and position distinctly expressed the intermolecular interaction existence. One can see that with increasing [acrylate] from step ***a*** to ***e*** [30], the fluorescence intensities of PN-**1** are enhanced concomitant redshifted peaks from 532–576 nm (see Fig. 6A). Noted that the concentrations of PN-**1** are the same (3.3×10^{-6} mol dm^{-3}) while those of acrylate are increased from step ***a*** to ***e***. The fact of the increasing fluorescence from ***a*** to ***e*** can be interpreted the molecular rotation suppressing and the complanation resulting from the solvent viscosity. Continuing addition of acrylate into the solution from step ***e*** to ***i*** [31], however, the fluorescence quenching was observed, with the position blueshifted, implying that the interactions within steps (***e***–***i***) and (***a***–***e***) are different. These can be confirmed by the corresponding fluorescence excitation spectra (see Fig. 6B). Firstly, one can see that PN-**1** displayed dual-fluorescence excitation peaks locating at ~350 nm and ~450 nm, similar to the absorption spectra (Fig. 2, left). From step ***a*** to ***e*** (Fig. 6B), the intensities in fluorescence excitation spectra were increased up to the maximum; and then rapidly decreased from ***e*** to ***i***. Meantime, the dual-fluorescence spectra locating at ~350 nm and ~450 nm metamorphose to the single fluorescence located at 420 nm. Evidently, the amount of acrylate resin have markedly different influence upon the chromophore: that is, the fluorescence of PN-**1** shows enhancement when [acrylate] is less than 75% (*V*%); further increasing [acrylate], the fluorescence decreases, accompanying the changes of maximum position and shape. Similar results of PN-**2** and PN-**3** have been presented in Fig. 6C–F. Although the emission quenching does not imply the photoinitiation, emission quenching is the consequence of strong interaction between monomer and initiator, such as photoinitiation [10,32]. Since the HOMO–LUMO gap of chromophores (2.45–2.54 eV) (see Table 1) is less than that of MMA monomer (4.1 eV) [33] the energy-transfer from the former to monomer is forbidden. Considering that two-photon absorbing chromophores usually exhibit large dipolar moment change ($\Delta\mu_{ge}$), according to Lippert–Mataga relationship (Eq. (2)), and strong intramolecular charge-transfer [29]. they would possess strong intermolecular charge-transfer. This is reasonable since the influence of matrix, expressed by the orientation polarizability (Δf) in Lippert–Mataga equation (Eq. (2)), is considered. So, on the assumption that two-photon induced polymerization (TPP) is initiated by the charge-transfer from TPA initiator and monomer, that is, chromophore firstly generates the exciton via two-photon absorption and then transfers charge to acrylate monomer, finally induces the later to polymerize.

4. Conclusions

New D–π_3–$(A)_{1-3}$ multibranched chromophores (PN-**1**, PN-**2** and PN-**3**) with triphenylamine as electron donor, naphthaline as bridge, and pyridyl ring as electron acceptor have been designed and synthesized as two-photon polymerization (TPP) initiators. Linear and nonlinear optical properties, including Lippert–Mataga equation, showed that the intramolecular and intermolacular interaction occurred, the former has contrition to TPA while the later helps to photoinitiation. Although all chromophores in this study have three branches, the increasing vinylpyridine groups from PN-**1**, PN-**2** and to PN-**3** decrease the molecular fluorescence quantum yield, which is desired for photoinitiation. The threshold powers of chromophores (~1.3 mW) were much lower than that of commercial benzil (7.5 mW) under identical experimental conditions. Microstructures of micro-ox size of 15 μm × 10 μm and microstereolithography with 20 μm × 20 μm bulk size and 1 μm × 1 μm grid size were fabricated. Intermolecular charge-transfer from D–π_3–$(A)_n$ initiator to acrylate monomer was deduced within the two-photon polymerization reaction, proved by the fluorescence quenching, electrochemistry measurements and Lippert–Matag equation

Acknowledgements

The authors are grateful to the National Natural Science Foundation of China (Grant Nos. 50673070, 50973077 and 50773091), Key Project of Chinese Ministry of Education (No. 204053),The National Basic Research Program of China (2010CB934103), and Science and technology development Project of Suzhou (SYJG0931) for financial supports.

References

[1] Gu J, Wang YL, Chen WQ, Dong XZ, Duan XM, Kawatac S. Carbazole-based 1D and 2D hemicyanines: synthesis, two-photon absorption properties and application for two-photon photopolymerization 3D lithography. New Journal of Chemistry 2007;31:63–8.
[2] Klein S, Barsella A, Leblond H. One-step waveguide and optical circuit writing in photopolymerizable materials processed by two-photon absorption. Applied Physics Letters 2005;86:211118.
[3] Kewitsch AS, Yariv A. Self-focusing and self-trapping of optical beams upon photopolymerization. Optics Letters 1996;21:24–6.
[4] Diamond C, Boiko Y, Esener S. Two-photon holography in 3-D photopolymer host-guest matrix. Optics Express 2000;6:64–8.
[5] Serbin J, Egbert A, Ostendorf A, Chichkov BN, Houbertz R, Domann G, et al. Femtosecond laser-induced two-photon polymerization of inorganic–organic hybrid materials for applications in photonics. Optics Letters 2003;28:301–3.
[6] Sun HB, Kawakami T, Xu Y, Ye J-Y, Matuso S, Misawa H, et al. Real three-dimensional microstructures fabricated by photopolymerization of monomer through two-photon absorption. Optics Letters 2000;25:1110–2.
[7] Wang I, Bouriau M, Baldeck PL, Martineau C, Andraud C. Three-dimensional microfabrication by two-photon-initiated polymerization with a low-cost microlaser. Optics Letters 2002;27:1348–50.
[8] Pudavar HE, Joshi MP, Prasad PN, Reinhardt BA. High-density three-dimensional optical data storage in a stacked compact disk format with two-photon writing and single photon readout. Applied Physics Letters 1999;74:1338–40.
[9] Bhawalkar JD, He GS, Prasad PN. Nonlinear multiphoton processes in organic and polymeric materials. Reports on Progress in Physics 1996;59:1041–70.
[10] Cumpston BH, Ananthavel SP, Barlow S, Dyer DL, Ehrlich JE, Erskine LL, et al. Two-photon polymerization initiators for three-dimensional optical data storage and microfabrication. Nature 1999;398:51–4.
[11] Xing JF, Chen WQ, Gu J, Dong XZ, Takeyasu N, Tanaka T, et al. Design of high efficiency for two-photon polymerization initiator: combination of radical stabilization and large two-photon cross-section achieved by N-benzyl 3,6-bis (phenylethynyl)carbazole derivatives. Journal of Materials Chemistry 2007;17:1433–8.
[12] Dong Y, Yu XQ, Sun YM, Hou XY, Li YF, Zhang X. Refractive index-modulated grating in two-mode planar polymeric waveguide produced by two-photon polymerization. Polymers for Advanced Technologies 2007;18:519–21.
[13] Zhang X, Yu XQ, Zhang BQ, Feng YG, Tao XT, Jiang MH. Synthesis and nonlinear optical properties of a new two-photon polymerization initiator: DPAMOB with a large TPA cross-section. Chinese Journal of Chemistry 2006;24:701–4.
[14] Li DM, Zhou HP, Pu JQ, Feng XJ, Wu JY, Tian YP, et al. Synthesis, luminescence and electrochemical properties of two phenothiazine derivatives. Chinese Journal of Chemistry 2005;23:1483–9.
[15] Watanabe T, Akiyama M, Totani K, Kuebler SM, Stellacci F, Wenseleers W, et al. Photoresponsive hydrogel microstructure fabricated by two-photon initiated polymerization. Advanced Functional Materials 2002;12:611–4.
[16] Heller C, Pucher N, Seidl B, Kalinyaprak K, Ullrich G, Kuna L, et al. One- and two-photon activity of cross-conjugated photoinitiators with bathochromic shift. Journal of Polymer Science: Part A: Polymer Chemistry 2007;45:3280–91.
[17] Lee KS, Yang DY, Park SH, Kim RH. Recent developments in the use of two-photon polymerization in precise 2D and 3D microfabrications. Polymers for Advanced Technologies 2006;17:72–82.

[18] Belfield KD, Schafer KJ, Liu Y, Liu J, Ren XB, Stryland EWV. Multiphoton-absorbing organic materials for microfabrication, emerging optical applications and non-destructive three-dimensional imaging. Journal of Physical Organic Chemistry 2000;13:837–49.
[19] Bratton D, Yang D, Dai J, Ober CK. Recent progress in high resolution lithography. Polymers for Advanced Technologies 2006;17:94–103.
[20] Beljonne D, Wenseleers W, Zojer E, Shuai Z, Vogel H, Pond SJK, et al. Advanced Functional Materials 2002;12:631–41.
[21] Hua YJ, Crivello JV. Macromolecules 2001;34:2488–94.
[22] Wang XM, Yang P, Jiang WL, Xu GB, Guo XZ. Strong two-photon absorption and two-photon excited fluorescence emission of heterofluorene derivatives. Optical Materials 2005;27:1163–70.
[23] Ohulchanskyy TY, Donnelly DJ, Detty MR, Prasad PN. Journal of Physical Chemistry B 2004;108:8668–72.
[24] Berberan-Santos MN, Garcia JM. Journal of the American Chemical Society 1996;118:9391–4.
[25] Albota MA, Xu C, Webb WW. Two-photon fluorescence excitation cross-sections of biomolecular probes from 690 to 960 nm. Applied Optics 1998;37:7352–6.
[26] Xia CJ, Advincula RC. Ladder-type oligo(*p*-phenylene)s tethered to a poly (alkylene) main chain: the Orthogonal approach to functional light-emitting polymers. Macromolecules 2001;34:6922–8.
[27] Wang XM, Yang P, Xu GB, Jiang WL, Yang TS. Two-photon absorption and two-photon excited fluorescence of triphenylamine-based multibranched chromophores. Synthetic Metals 2005;155:464–73.
[28] Wang XM, Zhou YF, Yu WT, Wang C, Fang Q, Jiang MH, et al. Two-photon pumped lasing stilbene-type chromophores containing various terminal donor groups: relationship between lasing efficiency and intramolecular charge transfer. Journal of Mathematical Chemistry 2000;10:2698–703.
[29] Wang ZM, Wang XM, Zhao JF, Jiang WL, Ping Yang, Fang XY, et al. Cooperative enhancement of two-photon absorption based on electron coupling in triphenylamine-branching chromophores. Dyes and Pigments 2008;79:145–52.
[30] In steps (***a***–***d***), the concentrations of PN- **n** (**n** = 1 or 2 or 3) are at 3.3×10^{-6} (mol dm^{-3}) in the presence of acrylate resin (the mixtures of methyl acrylate and dipentaerythritol hexaacrylate with equal weight) with different *V*%: that is, ***a***: 0; ***b***: 16.67%; ***c***: 33.33%; ***d***: 66.67%. The solvent is CH_2Cl_2.
[31] In steps (***e***–***l)***, the concentrations of acrylate resin (V%) and PN- **n** (mol dm^{-3}) are as follows: ***e***: [acrylate] = 75%, [PN- **n**] = 2.5×10^{-6}; ***f***: [acrylate] = 80%, [PN- **n**] = 2.0×10^{-6}; ***g***: [acrylate] = 85%, [PN- **n**] = 1.4×10^{-6}; ***h***: [acrylate] = 95%, [PN- **n**] = 4.0×10^{-7}; ***i***: [acrylate] = 99%, [PN- **n**] = 1.0×10^{-7}. The solvent is CH_2Cl_2.
[32] Nguyen LH, Straub M, Gu M. Acrylate-based photopolymer for two-photon microfabrication and photonic applications. Advanced Functional Materials 2005;15:209–16.
[33] Nicholas CS, Anzar K, Shannon WB, Alexander AM, Craig JH, Thuc-Quyen N, et al. One- and two-photon induced polymerization of Methylmethacrylate using colloidal CdS semiconductor quantum dots. Journal of the American Ceramic Society 2008;130:8280–8.